Title: A Novel Algorithm using Within-leg Calibration for Enhanced Accuracy of Detection of Arthritis by Infrared Thermal Imaging in Children

Authors: Yongdong Zhao, MD, PhD[1,2]; Ramesh S. Iyer, MD[3]; Mahesh Thapa, MD[3]; Debosmita Biswas, MS[4]; Nivrutti Bhide[2], Joshua Scheck, BS[1,2], Kevin Cain, PhD[5]; Savannah C. Partridge, PhD[4]; Carol A. Wallace, MD[1]

[1] Pediatric Rheumatology, Seattle Children's Hospital, Department of Pediatrics, University of Washington, Seattle, WA

[2] Center for Clinical and Translational Research, Seattle Children's Research Institute, Seattle, WA

[3] Department of Radiology, Seattle Children's Hospital, Seattle, WA

[4] Department of Radiology, University of Washington, Seattle, WA

[5] Department of Statistics, School of Nursing, University of Washington, Seattle, WA

Corresponding author:

Yongdong Zhao, MD, PhD

MA 7.110, 4800 Sand Point Way NE,

Seattle, WA 98105

Yongdong.zhao@seattlechildrens.org

Key words: Juvenile idiopathic arthritis, infrared thermal imaging, ultrasound, knee, ankle

Running title: Thermal imaging in JIA.

Abstract (word limit 250 words)

Objective: To standardize and improve the accuracy of detection of arthritis by thermal imaging.

Methods: Children with clinically active arthritis in the knee or ankle, as well as healthy controls, were enrolled to the development cohort and another group of children with knee symptoms were enrolled to the validation cohort. Ultrasound was performed for the arthritis subgroup for the development cohort. Joint exam by certified rheumatologists was used as a reference for the validation cohort. Infrared thermal data were analyzed using a custom software. Temperature after within-limb calibration (TAWiC) was defined as the temperature differences between joint and ipsilateral mid-tibia. TAWiC of knees and ankles was evaluated using ANOVA across subgroups. Optimal thresholds were determined by receiver operating characteristic (ROC) analysis using Youden index.

Results: There were significant differences in mean and 95th TAWiC of knee in anterior, medial, lateral views, and of ankles in anterior view, between inflamed and uninflamed counterparts ($p<0.05$). The area under the curve (AUC) was higher by 36% when using

$TAWiC_{Knee}$ than those when using absolute temperature. Within validation cohort, the sensitivity of accurate detection of arthritis in knee using both mean and 95th TAWiC from individual views or combined all 3 views ranged from 0.60 to 0.70 and the specificity was greater than 0.90 in all views.

Conclusion: Children with active arthritis or tenosynovitis in knees or ankles exhibited higher TAWiC than healthy joints. Our validation cohort study showed promise of the clinical utility of infrared thermal imaging for arthritis detection.

INTRODUCTION

Juvenile idiopathic arthritis (JIA) is the most common rheumatic disease in children (1). The most commonly affected joints are knees and ankles, followed by wrists and elbows (2). Early diagnosis and aggressive treatment are critical for maintaining normal joint functions in the management of JIA (3). A joint exam performed by a pediatric rheumatologist is considered standard assessment for children with JIA. Musculoskeletal ultrasound is more sensitive for joint synovitis than physical exam, but may also be limited by accessibility to equipment and by operators (4).

Infrared thermal imaging is a quick and noninvasive tool that can detect temperatures of different body parts with precision. It has been evaluated as a screening or supplementary tool for detecting or following up active arthritis in animal models (4,5), osteoarthritis (6,7), rheumatoid arthritis (8,9), and JIA (10–12). Studies focusing on larger joints (knees, ankles, wrists) (8,11,12) defined regions of interest (ROIs) based on anatomic location and reported absolute temperatures for comparison. Lasanen *et al.* showed significantly higher temperatures in inflamed ankles than controls but failed to confirm the difference between inflamed and healthy knee joints (11). Heat distribution index (HDI) was reported as another approach with a cutoff of 1.3°C to distinguish active arthritis in finger joints and wrists with a sensitivity of 67% and a specificity of 100% (8). Ilowite *et al.* (12) used the difference between inflamed joints and adjacent tissues in patients with symmetric arthritis. The temperature difference was associated with disease activity score (12). However, “adjacent tissue” was not clearly defined in that paper.

Our group has developed a standardized ROI definition approach in lower extremities for analysis of thermal images from children with chronic nonbacterial osteomyelitis (13). Our objectives were: 1) to enhance the sensitivity and reliability of detecting arthritis by using within-limb calibration for thermal imaging analysis; 2) to determine the threshold using within-limb calibration in children with known arthritis; 3) to validate this approach in new patients.

MATERIALS AND METHODS:

Institutional review board (IRB) approval (#15350, #1383) was obtained from the authors' tertiary-care, multidisciplinary pediatric hospital prior to the study. For the development cohort, two groups, including children with clinically confirmed arthritis in the knee or ankle, and healthy children between ages of 2 and 18 years, were consented and enrolled. Inclusion criteria of the arthritis group were active arthritis in knee and/or ankle diagnosed by treating physician (swelling, or pain with and limitations in motion if there was no swelling). Inclusion criteria of the healthy control group were normal skeletal health. Exclusion criteria for both groups were: 1) skin infection in imaged area that could interfere with thermal imaging results, 2) fever, 3) joint contracture greater than 10 degrees, and 4) inability to cooperate with the acquisition of thermal imaging, and 5) recent injury to the areas of interest. For the validation cohort, children with knee pain and/or swelling for at least a week, who seek care from rheumatology for the first time, were enrolled. The same exclusion criteria were applied as for the development cohort.

Image acquisition

Thermal Imaging Acquisition

As previously described (13), all subjects received infrared thermal imaging analysis of the lower limbs from four views (anterior, posterior, medial and lateral). Thermal imaging was performed using a Fluke™ TiR32 Thermal Imager (Fluke Inc., Everett, WA) with 76,800 pixels (320 x 240) (detection range -20 to 150 °C, sensitivity ≤0.04 °C) by trained staff to ensure sharp focus and consistent camera leveling and stabilization. The entire imaging session for each patient took less than 5 minutes. Subjects exposed their feet and entire legs to room air and rested for at least 10 minutes prior to imaging to allow stabilization and equilibration of skin temperature. Ambient temperature was set at 22.2 °C for all patients. Subjects posed in standardized positions to ensure consistency of image acquisition. Imaging was performed with subjects standing on a carpet to avoid influence from the cold floor on body temperature, and away from potentially interfering items such as metal panels, door knobs, computer screens, and adjacent people. Camera is positioned at the knee level of the subjects. The distance between camera and subject ranged between 4 to 5 m in order to maximize the spatial resolution of imaged body parts.

Ultrasound Imaging Acquisition

Only subjects from JIA group within the development cohort were scanned with ultrasound. Standard B-mode views of the knees (longitudinal and transverse suprapatellar, transverse posterior) with 20-30 degrees of flexion, tibiotalar joints (anterior longitudinal and transverse, medial and lateral paramalleolus) with plantar flexion, subtalar joints (lateral longitudinal) in neutral position, without compression were

collected after thermal imaging in the arthritis group by one pediatric rheumatologist (YZ) with USSONAR (Ultrasound School of North American Rheumatologists) certification and 5 years of experience using the GE LOGIQ e ultrasound machine (General Electronics Inc., Boston, MA). Matching joint examinations were performed on the same day before ultrasound images were obtained.

Subjects within the validation cohort were not scanned by ultrasound because the goal of applying this thermal imaging tool is to identify patients from community to accelerate the referral process and a joint exam performed by certified rheumatologist remains the well-accepted standard clinical practice.

Analysis of thermal images

The spatial and temperature data from infrared thermal images were exported from Smartview® software (Fluke Inc., Everett, WA). Data were then analyzed using customized semi-automated software developed in Matlab® (Mathworks, Natick, MA) as previously reported (13). In brief, lower legs were divided equally into three segments (proximal, mid, and distal) longitudinally by placing crosshairs at the medial and lateral sides of the knees and ankles from each view, and distal femur was defined as the same length as the proximal tibia/fibula segment. Then the proximal tibia/fibula and distal femur segments were merged as the ROI for knee. Using the distal tibia/fibula length as a reference, one-third of the reference above ankle line and one-ninth of the reference below the ankle line were merged as “ankle” for thermal imaging analysis that include tibiotalar and subtalar joints. Mean and 95th percentiles temperatures were recorded for each leg or joint segment. A previous study showed high reproducibility for

this technique (ICC 0.936-0.981) (13).

Temperature After Within-limb Calibration (TAWiC) was calculated as the summary measure (mean or 95th percentile) for the joint (knee or ankle) minus the summary measure for mid-tibia. Thus, TAWiC measures how much hotter the joint is than the mid-tibia of the same limb.

Ultrasound Reading

A small set of ultrasound images from previous patients were reviewed by two radiologists (RSI and MT) and a rheumatologist (YZ) for calibration purposes. Ultrasound images were scored as a consensus between two pediatric musculoskeletal radiologists (RSI, MT). When bone and tendon landmarks were not well visualized, images were excluded. A joint effusion was defined as anechoic material within the joint space or within the suprapatellar bursa (knee), or that displaced a fat pad in the tibiotalar and subtalar joints, as previously reported (15). Grading of joint effusion was performed as previously published (15,16). Synovial thickening was defined as hypoechoic material within the joint space that was not compressible. Tenosynovitis was defined as anechoic or hypoechoic material within the tendon sheath that circumscribed the tendon. Presence or absence of these parameters was recorded. Arthritis was defined as the presence of synovial thickening, or at least a moderate effusion without synovial thickening. Since it was difficult to distinguish tibiotalar and subtalar joints on thermal imaging, these are combined: the “ankle” was considered to be inflamed if either tibiotalar or subtalar joint (or both) was inflamed, or isolated tenosynovitis was present.

Demographic, clinical and laboratory data collection

Demographic information including gender, age, ethnicity, and race, and clinical data including body height, weight, oral or temporal temperatures were collected in all subjects. Within the JIA group in the development cohort and new patients in the validation cohort, the presence or absence of joint swelling, pain or warmth, physician global assessment (0-10), childhood health assessment questionnaire (CHAQ) score (0-3), patient/parent assessment of arthritis activity (0-10), patient/parent assessment of overall health (0-10), and current medications were recorded. Laboratory data including were also collected if available.

Data analysis

Histograms were examined for outliers and non-normality. Demographic variables were summarized and compared between children with JIA and healthy subjects using Chi-square tests for categorical measures and t-tests or Mann-Whitney U tests for numerical measures, depending on whether the measure is approximately normally distributed. Generalized estimating equations analysis was used to compare inflamed to uninflamed joints while accounting for the fact that the two joints within a child were not independent observations and using the sandwich estimator of standard error which is robust to non-normality. Absolute temperatures and TAWiC were dependent variables and whether or not the joint was inflamed was the predictor of interest. Analyses were done separately for each view. Receiver operating characteristic (ROC) curve analyses were used to describe how well the different summary measures can predict whether a joint is inflamed. Optimal thresholds were

determined by ROC analysis using Youden index then applied to the validation cohort. Sensitivity and specificity of detecting knee arthritis in validation cohort was determined using derived thresholds. Pearson correlation is used to describe the association between TAWiC 95 and demographic measures gender, age, height, weight and BMI. A P value below 0.05 was considered statistically significant. All analyses were done using IBM SPSS Version 19 (IBM Corp. Released 2010. IBM SPSS Statistics for Windows, Version 19.0. Armonk, NY: IBM Corp.)

A conservative power analysis showed that a sample size of 25 subjects per group would give over 90% power for detecting group differences as long as the true standardized effect size (difference in means divided by within-group SD) was at least 1.0. This effect size corresponds approximately to sensitivity of 70% and specificity of 70%. Since a measure with sensitivity and specificity smaller than this would not be useful clinically, this study has adequate power for detecting any clinically useful difference

RESULTS

Demographic characteristics

Fifty-three children from the JIA group, forty-nine from the healthy group from the development cohort, forty-three children with knee symptoms from the validation cohort were enrolled. Fifty-one children within the JIA group completed ultrasound examinations and had evaluable thermal imaging and were included in the analysis. Forty-eight children from the healthy group had evaluable thermal imaging and included

in the analysis. Patient characteristics from each group were summarized and compared in **Table 1**. There was no statistically significant difference in demographic characteristics between JIA and control groups. Within the JIA group, the mean duration of disease was three years, and a majority of subjects were not on systemic medications. The majority of JIA patients (65%) in development cohort were categorized as oligoarticular.

Physical exam and ultrasound results

Active arthritis on joint exam was defined as pain of motion (POM) plus limitation of motion (LOM), or swelling, for knee and ankle, and tenderness and POM, or tenderness and LOM for subtalar joint (17). Active arthritis on ultrasound was based on the presence of synovial thickening with or without effusion, or at least a moderate effusion if without synovial thickening for all three joints. Tenosynovitis around ankle and subtalar joints was classified as “inflammation of ankle” on ultrasound. Within the JIA group, 49 (48%) knee, 24 (22%) tibiotalar, and 15 (15%) subtalar joints had active arthritis on *physical examination*. Meanwhile, 45 (44%) knee, 15 (14%) tibiotalar, 11 (11%) subtalar joints had active arthritis and 8 (8%) ankle joints had active tenosynovitis on *ultrasound*. The final count of inflammatory knees was 45, and number of inflammatory ankles was 19. A total of 11 joints (knees or ankles) from development cohort were excluded from the analysis due to physical exam findings of arthritis but a normal ultrasound. Among 43 children with knee complaints within the validation cohort, seven patients had arthritis in a total of 10 knees whereas only three patients had arthritis in five ankles (tibiotalar and/or subtalar joint) determined by physical exam

alone.

Performance of thermal imaging analysis for detecting arthritis in development cohort

Within the development cohort, all joint segments (knee and ankle) were divided into three groups: the healthy control group, joints in the JIA group with inflammation, and joints in the JIA group without inflammation. Joints that were classified as arthritis by joint exam but not confirmed by ultrasound were excluded (**Supplements 1-3** showed results when joint exam as the only confirmation of arthritis). Preliminary analyses showed little difference between uninflamed joints in children with JIA and in healthy control children, so these two groups were combined into one group for all analyses, referred to as the uninflamed joint group. **Figure 1** revealed a representative patient with thermal image, absolute temperatures and TAWiC of knees, ankles and mid-tibia as well as corresponding ultrasound findings confirming active arthritis in a knee and a tibiotalar joint. **Table 2** showed means and standard deviation (SD) of the absolute and calibrated temperature summaries by inflammation status of joints from development cohort. The size of ROI showed trends of increase in inflamed limb but no statistically significant difference (Supplement 4).

Comparison of area under the curve using TAWiC versus absolute temperature

In general, absolute and TAWiC temperatures were higher in inflamed knees and ankles than in uninflamed counterparts. Compared to absolute values, TAWiC showed a greater temperature difference between groups, with smaller SD within each group and more significant p-values. Posterior view showed considerably a smaller difference

between groups than did the other views. Both TAWiC 95th percentile and mean temperatures of the inflamed knees from the anterior, lateral and medial views differed from the uninflamed knees by about 1 ^{0}C. However, TAWiC 95th percentile temperatures of the inflamed ankles differed from the uninflamed ankles more than TAWiC mean temperature did (0.88 vs. 0.42 ^{0}C). The temperatures of mid-tibia (a reference ROI for computing TAWiC) were slightly cooler in limbs corresponding to an inflamed joint, though this difference was not statistically significant.

ROC analyses using $TAWiC_{Knee}$ showed that the area under the curve (AUC) was similar among anterior, medial, and lateral views, but much lower in posterior views (**Table 3**). AUC was increased by 0.2 (30%) when $TAWiC_{knee}$ was used comparing to that of absolute temperature (ranging from 0.544-0.659). The thresholds of $TAWiC_{Knee}$ which maximizes Youden index were similar for anterior, medial, and lateral views (Table 3). The sensitivity of detecting arthritis in the knee varied from 0.64 to 0.78 and the specificity ranged between 0.79 and 0.92 excluding posterior view. The sensitivity of detecting inflammation in ankle region from anterior view was 0.80 and the specificity was 0.60. Other views of ankle, using our ROI definition, repeatedly spilled outside of limb contours and therefore was not evaluable. These results were similar to that from analyses completed with joint exam as the gold standard (Supplements 1-3) or ultrasound alone as the gold standard (Supplements 5-6).

Factors correlated with TAWiC

Correlations of 95th percentile TAWiC with gender, age, height, weight and BMI are shown in **Table 4**. Within the inflamed knee group, females had higher $TAWiC_{Knee}$

than males, and younger children and shorter children had higher $TAWiC_{Knee}$ than their older and taller counterparts, respectively. Within the inflamed ankle group, there was no correlation of $TAWiC_{Ankle}$ with gender, age, height, weight or BMI. However, within the healthy group, males, younger children and those with higher BMI had higher $TAWiC_{Ankle}$ whereas younger and shorter children without inflamed ankles in JIA group had higher $TAWiC_{Ankle}$.

Validation of using TAWiC to detect arthritis in the knee

Within the validation cohort, a knee joint was considered inflamed when both mean and 95th $TAWiC_{knee}$ of each knee were greater than the corresponding thresholds from each view in the development cohort. Comparing to the results of physical exam as the gold standard, the sensitivity of accurate detection of arthritis from individual views ranged from 0.60 to 0.70 and the specificity was greater than 0.9 in all views (**Table 5**). When all mean and 95th TAWiC readings from every view must be greater than the corresponding thresholds of corresponding views, the sensitivity and specificity were similar to using individual views (Table 5). Although the study was not designed to validate the detection of ankle inflammation, the sensitivity of using $TAWiC_{ankle}$ for detection was 0.80 and the specificity was 0.68.

DISCUSSION

This is the first study to propose a novel algorithm to reliably detect active arthritis in children using Infrared Thermal Imaging. Our approach to analyzing the thermal images from children with JIA and healthy children is reproducible and semi-

automated, making it potentially useful in a wide range of situations to detect active arthritis. The addition of the within-leg internal control in this investigation improved the capacity of distinguishing between inflamed and uninflamed joint area over an absolute temperature measure of the area of interest. This was a proof-of-concept study that focused on lower extremities due to the high prevalence of arthritis in knees and ankles. Further refinement of this approach may be applied to disease monitoring of chronic arthritis in both adults and children.

We identified significantly increased temperatures in both inflamed knee and ankle joints not only by absolute temperature as other studies (10,11) but also reduced the variation significantly by applying within-limb calibration. Therefore, our algorithm greatly improved the distinguishing ability of arthritis by thermal imaging. In addition, the definition of the knee joint and ankle were based on anatomy and this principle can be applied to other joints such as elbow, wrist and digit joints. Another advantage of applying an internal control is to allow identification of joint inflammation in both legs of an affected individual.

Among all views, anterior, medial and lateral views provided similar sensitivity to distinguish knees with inflammation from those without inflammation, which is consistent with previous studies (10,11). For the ankle joint, due to greater anatomical complexity, articular or tendon sheath inflammation may cause temperature changes that are only detectable on certain views. In this analysis, only the anterior view showed a significant difference in $TAWiC_{Ankle}$ between inflamed and uninflamed ankles. Optimization of ROI for ankle joints from medial, lateral and posterior views might allow us to determine the

specificity of view-specific changes of temperatures that correspond to inflammation from specific anatomical structures. For example, isolated inflammation within lateral tendons may reveal elevated $TAWiC_{Ankle}$ only from a lateral view and not from other views. Definition of ankle ROI and patterns of heat distribution from other views may be defined and evaluated through a machine learning approach in the future.

The significant impact of age, gender and height on 95th $TAWiC_{Knee}$ and $TAWiC_{Ankle}$ in subgroups suggest that our method needs to be validated in various age groups, and that thresholds may be different depending on age and gender. It is also possible that the increase of TAWiC is dependent on the severity of joint swelling such that more subtle swelling is less detectable by thermal imaging. Using the current dataset from development cohort, we identified thresholds of TAWiC for equally maximized sensitivity and specificity. For practical use, one may select a higher threshold for greater specificity when the pre-test probability is low, such as screening of healthy children. In contrast, a lower threshold may be chosen for higher sensitivity when the pre-test probability is high, such as a child with history of JIA who has knee pain.

We validated the new algorithm and preliminary thresholds of $TAWiC_{knee}$ in a separate cohort that demonstrated reasonable sensitivity and high specificity. With modification of the threshold of mean $TAWiC_{knee}$, sensitivity can be increased from 0.70 to 0.90 without sacrificing specificity. These results showed promise of potentially applying thermal imaging in screening and monitoring knee arthritis in children especially during the era of increasing telehealth when joint exam is not performed in

person. However, in-person visit and established imaging such as MRI and ultrasound are still needed when persistent symptoms are concerning despite normal thermal imaging results.

Our study had several limitations. Our sample size was small, but comparable to previous studies, and exploratory statistics was performed without adjusting for multiple comparisons. Ankle ROI definition was not suitable for views other than anterior, which limits broader applicability. Finally, reproducibility of the temperature measurements over several days was not assessed due to difficulty in retaining subjects for repeat evaluations. However, we were able to prove that capacity of determining inflammation of knees and ankles by thermal imaging were increased when using internal calibration. Furthermore, the thresholds determined can effectively screen for arthritis with a reasonable sensitivity and high specificity. These findings, if validated in a large population with optimization, will be highly applicable to patient care, especially during telehealth.

CONCLUSION

The use of a novel algorithm of infrared thermal imaging in children with active arthritis, or tenosynovitis, in knees or ankles revealed higher TAWiC than healthy unaffected joints. Our validation cohort study showed promise of the clinical utility of infrared thermal imaging for arthritis detection.

Author contribution

All authors were involved in drafting the article or revising it critically for important

intellectual content, and all authors approved the final version to be published. Dr. Zhao had full access to all of the data in the study and takes responsibility for the integrity of the data and the accuracy of the data analysis.

ACKNOWLEDGEMENT

The authors would like to thank participants of the study, Ms. Ching Hung, Ms. Mary Eckert, Mr. Christopher Budech for their help with infrared thermal imaging, and Dr. Jeffrey Ojemann for graciously allowing study team to use the infrared thermal camera. We appreciate the guidance from Drs. Margret Rosenfeld, Dennis Shaw, Anne Stevens, Susan Halbach, David Suskind, and the referrals of patients from Drs. Matthew Basiaga, Sri Grevich, Kristen Hayward, Shaun Jackson, Kabita Nanda, Sarah Ringold, Susan Shenoi, Clayton Sontheimer, Anne Stevens, and Jennifer Turner. This study was supported by Clinical Research Scholar Program and Pilot Study Grant from Seattle Children's Research Institute. Yongdong Zhao's research is supported by Bristol-Meyer Squibb, American College of Rheumatology and European League Against Rheumatism, Washington Research Foundation and CARRA.

REFERENCES

1. Manners PJ, Diepeveen DA. Prevalence of juvenile chronic arthritis in a population of 12-year-old children in urban Australia. Pediatrics 1996;98:84-90.
2. Huemer C, Malleson PN, Cabral DA, Huemer M, Falger J, Zidek T, et al. Patterns of joint involvement at onset differentiate oligoarticular juvenile psoriatic arthritis from pauciarticular juvenile rheumatoid arthritis. J Rheumatol 2002;29:1531-5.
3. Wallace CA, Giannini EH, Spalding SJ, Hashkes PJ, Neil KMO, Zeft AS, et al. Trial of Early Aggressive Therapy in Polyarticular Juvenile Idiopathic Arthritis. Arthritis Rheum 2012;64:2012-21.
4. Brenner M, Braun C, Oster M, Gulko PS. Thermal signature analysis as a novel method for evaluating inflammatory arthritis activity. Ann Rheum Dis 2006;65:306-11.
5. Sanchez BM, Lesch M, Brammer D, Bove SE, Thiel M, Kilgore KS. Use of a portable thermal imaging unit as a rapid, quantitative method of evaluating inflammation and experimental arthritis. J Pharmacol Toxicol Methods 2008;57:169-75.
6. Varju G, Pieper CF, Renner JB, Kraus VB. Assessment of hand osteoarthritis: Correlation between thermographic and radiographic methods. Rheumatology 2004;43:915-9.
7. Denoble AE, Hall N, Pieper CF, Kraus VB. Patellar skin surface temperature by thermography reflects knee osteoarthritis severity. Clin Med Insights Arthritis Musculoskelet Disord 2010;3:69-75.

8. Spalding SJ, Kwoh CK, Boudreau R, Enama J, Lunich J, Huber D, et al. Three-dimensional and thermal surface imaging produces reliable measures of joint shape and temperature: a potential tool for quantifying arthritis. Arthritis Res Ther 2008;10:R10.

9. Snekhalatha U, Anburajan M, Sowmiya V, Venkatraman B, Menaka M. Automated hand thermal image segmentation and feature extraction in the evaluation of rheumatoid arthritis. Proc Inst Mech Eng H 2015;229:319-31.

10. Viitanen SM, Laaksonen AL. Thermography in Juvenile Rheumatoid Arthritis. Scand J Rheumatol 1987;16:91-8.

11. Lasanen R, Piippo-Savolainen E, Remes-Pakarinen T, Kroger L, Heikkila A, Julkunen P, et al. Thermal imaging in screening of joint inflammation and rheumatoid arthritis in children. Physiol Meas 2015;36:273-82.

12. Ilowite NT, Walco GA, Pochaczevsky R. Assessment of pain in patients with juvenile rheumatoid arthritis: relation between pain intensity and degree of joint inflammation. Ann Rheum Dis 1992;51:343-6.

13. Zhao Y, Iyer RS, Reichley L, Oron AP, Gove NE, Kitsch AE, et al. A Pilot Study of Infrared Thermal Imaging to Detect Active Bone Lesions in Children with Chronic Nonbacterial Osteomyelitis. Arthritis Care Res 2019;71:1430-5.

14. Laurell L, Court-Payen M, Nielsen S, Zak M, Fasth A. Ultrasonography and color Doppler in juvenile idiopathic arthritis: diagnosis and follow-up of ultrasound-guided steroid injection in the ankle region. A descriptive interventional study. Pediatr Rheumatol 2012;10:11.

15. Zhao Y, Rascoff NE, Iyer RS, Thapa M, Reichley L, Oron AP, et al. Flares of Disease in Children with Clinically Inactive Juvenile Idiopathic Arthritis Were Not Correlated with Ultrasound Findings. J Rheumatol 2018;45:851-7.

16. Ting T V., Vega-Fernandez P, Oberle EJ, De Ranieri D, Bukulmez H, Lin C, et al. Novel Ultrasound Image Acquisition Protocol and Scoring System for the Pediatric Knee. Arthritis Care Res 2019;71:977-85.

17. Wallace CA, Giannini EH, Huang B, Itert L, Ruperto N. American College of Rheumatology provisional criteria for defining clinical inactive disease in select categories of juvenile idiopathic arthritis. Arthritis Care Res (Hoboken) 2011;63:929-36.

Figure 1: Representative thermal image, ultrasound images and thermal analysis results from a child with arthritis (swelling on exam, effusion in ultrasound) in right knee and left ankle. Enclosed red lines on ultrasound indicate joint effusion. Significantly elevated temps vs reference region (mid-tibia) are shown in bold.

Table 1. Baseline characteristics of children in JIA group and control group

Variables Mean ± SD or number (%)	Development cohort JIA group (n=51)	 Healthy control (n=48)	 P value[$]	Validation cohort Unknown (n=43)
Age at enrollment (years)	9.0 ± 4.1	9.7 ± 3.4	0.40	10.7 ± 4.1
Female	33 (65)	33 (69)	0.42	27 (63)
Weight (kg)	36.6 ± 21.4	36.2 ± 18.7	0.91	43.8 ± 18.9
Height (cm)	133.1 ± 25.6	137.9 ± 20.4	0.31	144.2 ± 22.1
BMI	18.9 ± 4.7	17.9 ± 4.1	0.26	17.9 ± 4.1
Oral temperature (^{0}C)	36.8 ± 0.4 (N=15)	36.9 ± 0.3 (N=37)	0.41	37.0 ± 0.2
Race			0.06	
Caucasian	39 (77)	35 (73)		36 (84)
African American	3 (6)	3 (6)		1 (2)
Asian	2 (4)	9 (19)		0 (0)
Native American	0 (0)	1 (2)		1 (2)
Pacific islander	1(2)	0 (0)		0 (0)
Other	6 (12)	0 (0)		5 (12)
ILAR category				
Persistent oligoarticular	29 (57)	NA		3 (7)
Extended oligoarticular	4 (8)	NA		0 (0)
Rheumatoid-factor negative polyarthritis	9 (18)	NA		1 (2)
Rheumatoid-factor positive polyarthritis	1 (2)	NA		1 (2)
Enthesitis-related arthritis	3 (6)	NA		0 (0)
Psoriatic JIA	4 (8)	NA		0 (0)
Systemic JIA	1 (2)	NA		0 (0)
Undifferentiated JIA	0 (0)	NA		1 (2)
Disease duration at enrollment (years)	3.0 ± 3.6	NA		NA
Laboratory findings				
ANA positive	25 (49), (n=45)	NA		12 (48), (n=25)
RF positive	3 (6), (n=38)	NA		1 (5), (n=19)
CCP positive	1 (2), (n=33)	NA		2 (15), (n=13)
HLA-B27 positive	2 (4), (n=33)	NA		4 (31), (n=13)
Erythrocyte sedimentation rate, mm/h (normal 0-20) (n=34)	25.8 ± 26.0	NA		NA
Patient/parent reported measures				
Patient/parent's global assessment of overall health (range 0–10)	2.3 ± 2.3 (n=48)	NA		NA
Patient/parent's assessment of arthritis activity (range 0–10)	3.9 ± 2.8 (n=48)	NA		NA
CHAQ	0.5 ± 0.5 (n=50)	NA		0.8 ± 0.6 (n=43)
Physician global assessment (range 0-10)	2.6 ± 1.5 (n=40)	NA		NA
Treatment at study entry				
NSAIDs	18 (35)	NA		27 (63)
DMARD	15 (29)	NA		NA
Biologic	8 (16)	NA		NA
Systemic glucocorticoids	4 (8)	NA		1 (2)

ILAR: International League of Associations for Rheumatology, ANA: antinuclear antibody, RF: rheumatoid factor, CCP: cyclic citrullinated peptide, HLA: human leukocyte antigen, CHAQ: childhood health assessment questionnaire, NSAID: nonsteroidal anti-inflammatory drug, DMARD: disease-modifying antirheumatic drug, NA: not applicable. [$:] statistics between two groups within development cohort

Table 2. TAWiC from knee and ankle ROI in children with JIA group and healthy children

Variables	Inflamed joints (JIA), Mean ± SD	Uninflamed joints (JIA & control), Mean ± SD	p value
Analyses of Knees and Corresponding Mid Tibia	**N=45**	**N=142**	
Knee			
95th absolute (Anterior)	34.46 ± 1.20	33.76 ± 1.26	.002
95th absolute (Lateral)	34.03 ± .97	33.53 ± 1.05	.006
95th absolute (Medial)	33.96 ± 1.04	33.60 ± 1.20	.085
95th absolute (Posterior)	34.24 ± 1.03	34.28 ± 1.00	.811
95th TAWiC (Anterior)	1.02 ± .83	-.08 ± .50	<.001
95th TAWiC (Lateral)	1.15 ± .90	.17 ± .50	<.001
95th TAWiC (Medial)	1.27 ± .77	.28 ± .60	<.001
95th TAWiC (Posterior)	1.93 ± .85	1.64 ± .56	.08
Mean absolute (Anterior)	33.33± 1.27	32.71 ± 1.32	.01
Mean absolute (Lateral)	32.76 ±1.01	32.56 ± 1.11	.30
Mean absolute (Medial)	32.85 ± 1.07	32.65 ± 1.17	.35
Mean absolute (Posterior)	32.95 ± 1.02	33.01 ± 1.09	.75
Mean TAWiC (Anterior)	.67 ± .97	-.39 ± .56	<.001
Mean TAWiC (Lateral)	.72 ± .74	-.13 ± .52	<.001
Mean TAWiC (Medial)	.89 ± .76	.02 ± .60	<.001
Mean TAWiC (Posterior)	1.53 ± .73	1.22 ± .52	.025
Mid tibia			
95th absolute (Anterior)	33.44 ± 1.23	33.85 ± 1.21	.069
Mean absolute (Anterior)	32.66 ± 1.26	33.10 ± 1.26	.058
Analyses of Ankles and Corresponding Mid Tibia	**N=20**	**N=168**	
Ankle			
95th absolute (Anterior)	33.83 ± 1.55	33.55 ± 1.76	.50
95th TAWiC (Anterior)	.60 ± 1.19	-.28 ± 1.11	.002
Mean absolute (Anterior)	32.14 ± 1.55	32.23 ± 1.73	.798
Mean TAWiC (Anterior)	-.42 ± .73	-.84 ± .96	.019
Mid tibia			
95th absolute (Anterior)	33.23 ± 1.43	33.83 ± 1.15	.064
Mean absolute (Anterior)	32.56 ± 1.40	33.08 ± 1.20	.106

TAWiC: Temperature After Within-limb Calibration, ROI: region of interest,

Table 3. Area under the curve when using TAWiC or absolute temperatures from knee and ankle and thresholds derived by using TAWiC

Variables	AUC by TAWiC	AUC by absolute temp	Youden-maximizing threshold (C)	Youden index	sensitivity	specificity
Knee						
95th TAWiC (Anterior)	0.867	0.659	0.540	0.628	0.733	0.894
95th TAWiC (Lateral)	0.840	0.653	0.710	0.560	0.689	0.871
95th TAWiC (Medial)	0.846	0.587	0.805	0.583	0.733	0.85
95th TAWiC (Posterior)	0.590	0.474	1.900	0.207	0.488	0.728
Mean TAWiC (Anterior)	0.843	0.640	0.305	0.567	0.644	0.923
Mean TAWiC (Lateral)	0.843	0.558	0.270	0.585	0.778	0.800
Mean TAWiC (Medial)	0.815	0.544	0.463	0.504	0.711	0.793
Mean TAWiC (Posterior)	0.618	0.470	1.485	0.226	0.465	0.761
Ankle						
95th TAWiC (Anterior)	0.699	0.542	0.130	0.407	0.800	0.601
Mean TAWiC (Anterior)	0.637	0.425	-.720	0.276	.800	.476

TAWiC: Temperature After Within-limb Calibration, AUC: area under the curve, Youden index=sensitivity + specificity -1

Table 4. Correlation of gender, age, height, weight, BMI and body temperature with TAWiC_knee and TAWiC_ankle

Variables	Healthy control	Uninflamed joint (JIA)	Inflamed joint (JIA)
Anterior Knee	**N= 96**	**N=46**	**N=45**
Gender	.71 (.493)	.126 (.406)	.371 (.012)
Age	.0698 (.509)	-.156 (.302)	-.231 (.127)
Height	.090 (.383)	-.199 (.186)	-.204 (.179)
Weight	.128 (.215)	-.175 (.244)	.071 (.643)
BMI	.068 (.510)	-.147 (.328)	.014 (.930)
Lateral Knee	**N=94**	**N=46**	**N=45**
Gender	-.108 (.298)	.146 (.331)	.453 (.002)
Age	.032 (.757)	-.282 (.058)	-.324 (.030)
Height	.123 (.238)	-.261 (.079)	-.302 (.043)
Weight	.158 (.129)	-.198 (.187)	-.231 (.127)
BMI	.109 (.297)	-.073 (.628)	-.176 (.246)
Medial Knee	**N=94**	**N=46**	**N=45**
Gender	.094 (.368)	-.057 (.704)	.028 (.855)
Age	.142 (.171)	.027 (.857)	.013 (.932)
Height	.130 (.213)	-.-41 (.785)	.106 (.490)
Weight	.059 (.571)	.031 (.845)	.229 (.130)
BMI	-.062 (.553)	.012 (.938)	.208 (.171)
Posterior Knee	**N=96**	**N=46**	**N=43**
Gender	.236 (.020)	.056 (.712)	-.351 (.021)
Age	.077 (.454)	-.048 (.749)	.120 (.445)
Height	.067 (.517)	-.125 (.408)	.230 (.138)
Weight	.035 (.737)	.022 (.887)	.291 (.058)
BMI	-.040 (.696)	.080 (.596)	.150 (.338)
Anterior Ankle	**N=96**	**N=83**	**N=19**
Gender	-.206 (.045)	.006 (.954)	.243 (.315)
Age	-.220 (.031)	-.289 (.008)	-.233 (.337)
Height	-.089 (.386)	-.265 (.015)	-.200 (.412)
Weight	.145 (.159)	-.099 (.374)	-.053 (.830)
BMI	.307 (.002)	.134 (.226)	.107 (.663)

Values were expressed as correlation coefficient (p value). TAWiC: Temperature After Within-limb Calibration, US: ultrasoud, JIA: juvenile idiopathic arthritis

Table 5. Sensitivity and specificity of detection of arthritis in knee (n=43)*

Views	sensitivity (95% CI)	specificity (95% CI)
Anterior	0.60 (0.26-0.88)	0.91 (0.82-0.96)
Lateral	0.70 (0.35-0.93)	0.95 (0.87-0.99)
Medial	0.70 (0.35-0.93)	0.93 (0.85-0.98)
Anterior + lateral + medial**	0.60 (0.26-0.88)	0.99 (0.93-1.00)

*Definition of accurate detection by thermal imaging is made when the mean TAWiC (Temperature After Within-limb Calibration) of the knee is greater than the threshold for mean AND the 95th TAWiC of the knee is greater than the threshold for 95th temperature. **All Mean and 95th TAWiC readings from every view must be greater than the corresponding thresholds of corresponding views

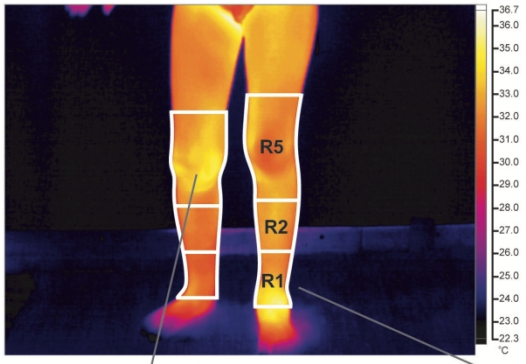

	Absolute 95th highest temp (°C)		TAWiC (°C)	
	L	R	L	R
Knee (R5)	33.3	**34.1**	0.6	**2.0**
Ankle (R1)	**34.2**	32.9	**1.5**	0.8
Mid-Tibia (R2)	32.7	32.1	Ref	Ref

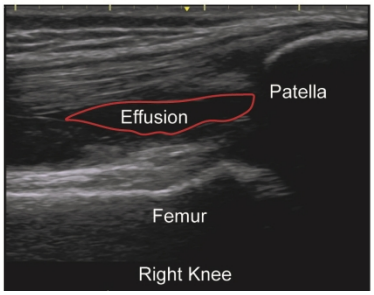

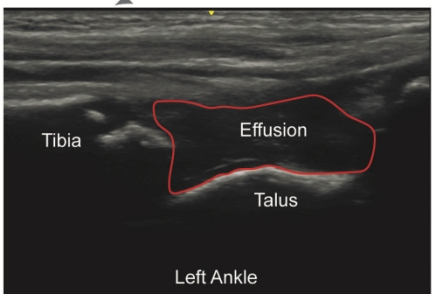

Figure 1.